

Investigation of Magnesium Ferrite Spinel Solid Solution with Iron-Rich Composition

N. M. Deraz¹ and Omar H. Abd-Elkader²

¹Physical Chemistry Department, Laboratory of Surface Chemistry and Catalysis, National Research Center, Dokki, Cairo, Egypt.

²Electron Microscope Unit, Zoology Department, College of Science, King Saud University, Riyadh 11451, Kingdom of Saudi Arabia.

Received: 2 May 2013 / *Accepted:* 12 June 2013 / *Published:* 1 July 2013

The structural and morphological properties of Mg- Fe- O system were determined by using X-ray diffraction (XRD), Scanning electron micrographs (SEM), Infrared (IR) and Energy dispersive X-ray (EDX) techniques. Combustion method resulted in formation Mg- Fe- O system in one step. The results revealed that the as prepared solids consisted entirely of well nano- crystalline spinel magnesium ferrite solid solution with iron-rich composition, $MgFe_2O_4 \cdot xFe_2O_3$, depending upon XRD data. SEM shows formation of nano- materials with sponge-like structure. The concentration of constituents, involved in the as synthesized material was determined by using EDX technique. In fact, it was found the concentration of Mg, Fe and O species changes from the uppermost surface layer to the bulk of the system studied.

Keywords: XRD; SEM; EDX; Fe_2O_3 ; $MgFe_2O_4$; Solid Solution.

1. INTRODUCTION

Due to the unique physical properties of ferrite based nano- crystalline materials, there are different applications of these materials such as catalysts, adsorptive solids, sensors, color pigments, magnetic recording medium, information storage, bio-processing and magneto-optical devices [1-5]. Actually, the ferrites can be used as stable pigments at high temperatures, above 1000 °C, to color up porcelain and ceramics [6, 7]. Among ferrite based pigments, magnesium ferrite ($MgFe_2O_4$) is nowadays commercially used as oil paint [8].

The traditional preparation of iron-rich pigments is solid state route with elevated temperature [9]. However, several wet chemical methods can be used to prepare of magnesium ferrite nanoparticles such as co-precipitation, supercritical drying processes, micelle routes and hydrothermal [10-

12]. Indeed, economical routes for production of large quantities of Mg ferrite are solid state reactions and co-precipitation. One of disadvantages of these routes is formation of undesired non-uniform particles due to the agglomeration of nano-particles.

Alternatively, one of efficient method for preparing nano-materials at moderate conditions is the combustion route. One authors reported that combustion method derived nano-particles possessed good chemical homogeneity, high purity and lower calcination temperature [13]. Glycine – assisted combustion technique led to prepare a single nano- magnetic magnesium ferrite phase in one step [13]. The morphological properties (grain size and shape) of the pigments can impact their coloration [14]. Indeed, low temperature routes allow a morphology control. In addition, the intense reddish-brown color observed in case of iron-rich materials is entirely due to the Fe^{3+} chromophore cation [14].

The nano-sized ceramic pigments have a massive potential market due to their high surface area. Preparation of ceramic pigments with particle size in the nano-scale brought about higher surface coverage, higher number of reflectance points with subsequent improved scattering. The nano-sized materials based paints have high mechanical strength due to the uniform dispersion of small particle size of pigment. However, the nano-sized pigments exhibit superior effectiveness also in critical abrasive and polishing applications [15].

Iron oxides hold a very important place in the pigment market because of their wide range of colors, stability, and nontoxic nature. Iron oxides based pigments resulted in four major colors that are browns, reds, blacks and yellows. In fact, the ferrite pigments are technically not iron oxides, but it can be included in the iron oxide family due to the similarity of characteristics and chemical compositions. Several authors reported recently that MgFe_2O_4 can also be efficient pigment for air or water purification due to its desirable properties in terms of photo-absorption and photo-corrosion resistance [16-18].

The aim of this work is to assess the structural and morphological properties of spinel magnesium ferrite solid solution with iron – rich composition. The employed techniques are X-ray diffraction (XRD), Scanning electron micrographs (SEM), Energy dispersive X-ray (EDX) and Infrared (IR) techniques..

2. EXPERIMENTAL

2.1. Powders Preparation

One sample of Fe/Mg mixed oxides was prepared by mixing non-stoichiometric proportions of iron and magnesium nitrates with calculated amount of glycine [13]. The ratio of the glycine: magnesium: ferric nitrates were 4: 0.5: 2. The mixed precursors were concentrated in a porcelain crucible on a hot plate at 400 °C for quarter hour. During heating the crucible, the crystal water was gradually vaporized. When a crucible temperature was reached to the critical temperature, large amounts of foams produced with appearance of spark at one corner which spread through the mass, yielding a voluminous and fluffy product in the container. The chemicals employed in the present work were of analytical grade supplied by Prolabo Company.

2.2. Characterization techniques

An X-ray measurement of mixed oxide solids was carried out using a BRUKER D8 advance diffractometer (Germany). The patterns were run with Cu K_{α} radiation at 40 kV and 40 mA with scanning speed in 2θ of $2^{\circ} \text{ min}^{-1}$.

The crystallite size of the produced MgFe_2O_4 particles was based on X-ray diffraction line broadening and calculated by using Scherrer equation [18].

$$d = \frac{B\lambda}{\beta \cos \theta} \quad (1)$$

where d is the average crystallite size of the phase under investigation, B is the Scherrer constant (0.89), λ is the wave length of X-ray beam used, β is the full-width half maximum (FWHM) of diffraction and θ is the Bragg's angle.

Scanning electron micrographs (SEM) was recorded on JEOL JAX-840A electron micro-analyzer. The sample was dispersed in ethanol and then treated ultrasonically in order to disperse individual particles over gold grids.

Energy dispersive X-ray analysis (EDX) was carried out on Hitachi S-800 electron microscope with an attached kevox Delta system. The parameters were as follows: accelerating voltage 15 kV, accumulation time 100s, window width $8 \mu\text{m}$. The surface molar composition was determined by the Asa method, Zaf-correction, Gaussian approximation.

An infrared transmission spectrum of various solids was determined using Perkin-Elmer Spectrophotometer (type 1430). The IR spectra were determined from 1000 to 400 cm^{-1} . Two mg of each solid sample were mixed with 200 mg of vacuum-dried IR-grade KBr. The mixture was dispersed by grinding for 3 min in a vibratory ball mill and placed in a steel die 13 mm in diameter and subjected to a pressure of 12 tonnes. The sample disks were placed in the holder of the double grating IR spectrometer.

3. RESULTS AND DISCUSSION

3.1. Formation of $\text{MgFe}_2\text{O}_4 \cdot x\text{Fe}_2\text{O}_3$ compound

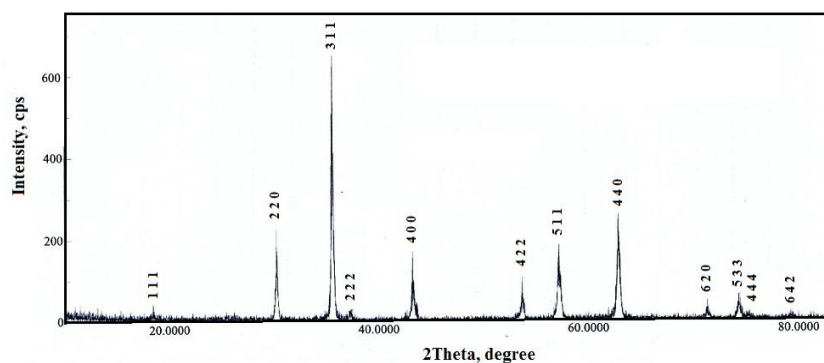


Figure 1. XRD pattern for Mg- Fe- O system.

Fig. 1 shows the XRD pattern for the as prepared sample. Study of this figure revealed that the as synthesized sample consisted entirely of magnesium ferrite, MgFe_2O_4 , nano- particles depending upon JCPDS card No. 17- 464. Various planes (1 1 1), (2 2 0), (3 1 1), (2 2 2), (4 0 0), (4 2 2), (5 1 1), (4 4 0), (6 2 0), (5 3 3), (4 4 4) and (6 4 2) have been determined. These planes are relative to the cubic spinel structure of magnesium ferrite with space group $Fd3m$ [23]. Indeed, the stoichiometric ratio for the Mg/Fe is 0.5 resulted in a single spinel MgFe_2O_4 phase [13]. In this study, The Mg/Fe ratio is 0.25 yielding an excess amount of iron oxide. In fact, XRD pattern shows no any second phase indicating probability presence the excess amount of iron oxide in amorphous phase and/or formation of Mg- Fe- O solid solution. However, presence of excess amount of iron oxide brought about formation of magnesium ferrite solid solution with iron- rich composition. The as prepared system has small crystallite size depending upon the low crystallinity of its particles.

The calculated values of the crystallite size (d), lattice constant (a), unit cell volume (V) and X-ray density (D_x) of MgFe_2O_4 nano- particles depending upon the data of X-ray are given in Table 1. It was found that the value of V and a of the as prepared magnesium ferrite are less than that present in JCPDS card No. 17- 464. This decrease could be attributed to incorporation of iron oxide in the crystal lattice of magnesium ferrite with contraction of its lattice depending upon the ionic radii of the reacting species ($\text{Fe}^{2+}=0.074$ nm, $\text{Fe}^{3+}=0.064$ nm and $\text{Mg}^{2+}=0.065$ nm) [24]. Opposite behavior was observed for X-ray density (D_x) of Mg ferrite. However, Table 2 displays the calculated values of the distance between the reacting ions (L_A and L_B), ionic radii (r_A , r_B) and bond lengths (A–O and B–O) on tetrahedral (A) sites and octahedral (B) sites of MgFe_2O_4 crystallites depending upon the data of X-ray.

Table 1. Some structural parameters for the as prepared Mg-Fe-O system.

Sample	d (nm)	a (nm)	V (nm^3)	D_x (g/cm^3)
$\text{MgFe}_2\text{O}_4 \cdot x\text{Fe}_2\text{O}_3$	25	0.8381	0.5887	4.5153

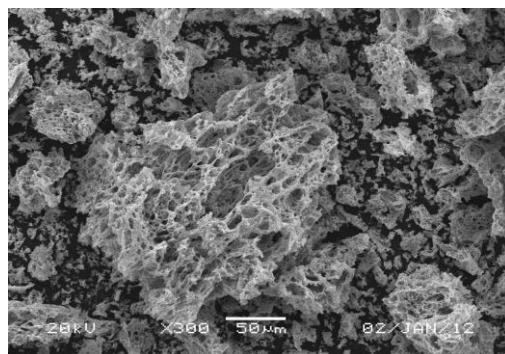
Table 2. The values of L_A , L_B , A-O, B-O, r_A and r_B for the as prepared Mg-Fe-O system.

Sample	L_A (nm)	L_B (nm)	A-O (nm)	B-O (nm)	r_A (nm)	r_B (nm)
$\text{MgFe}_2\text{O}_4 \cdot x\text{Fe}_2\text{O}_3$	0.3629	0.2963	0.2032	0.1969	0.0682	0.0582

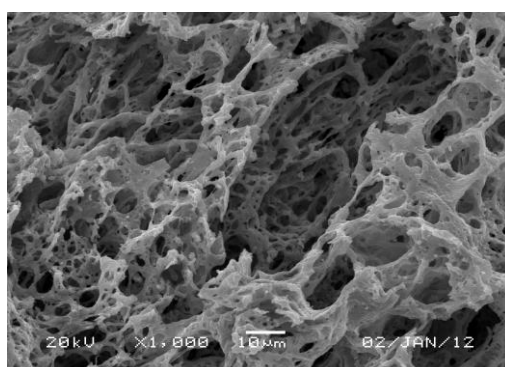
3.2. SEM study

Study the morphology of the as prepared sample was achieved by using SEM technique. SEM images with different magnifications for the Mg- Fe- O system are given in Fig. 2 A - D. These images display formation of spongy, homogeneous and fragile material. However, it can be seen from this

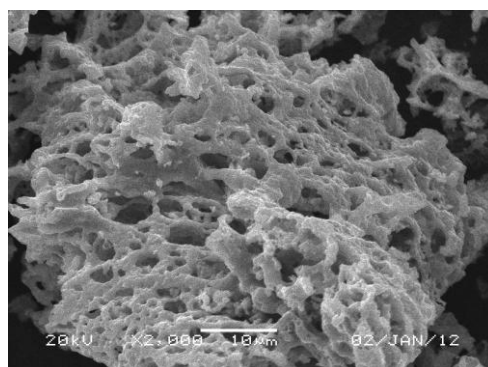
figure that the as prepared solid contains voids and pores depending upon large amount of gases during combustion process.



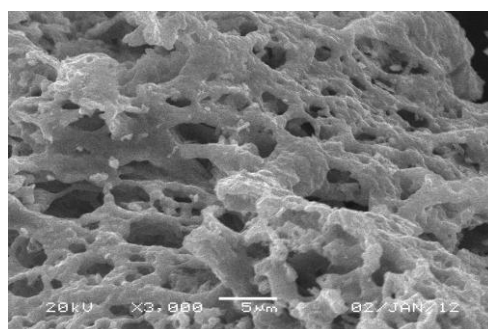
A



B



C



D

Figure 2. SEM images for the as prepared sample with different magnifications.

3.3. EDX analysis

Fig. 3 showed EDX spectrum of the Mg- Fe- O system at 20 keV. This spectrum displays the effective atomic concentrations of different constituents (Mg, Fe and oxygen species) on top surface layers of the Mg- Fe- O system.

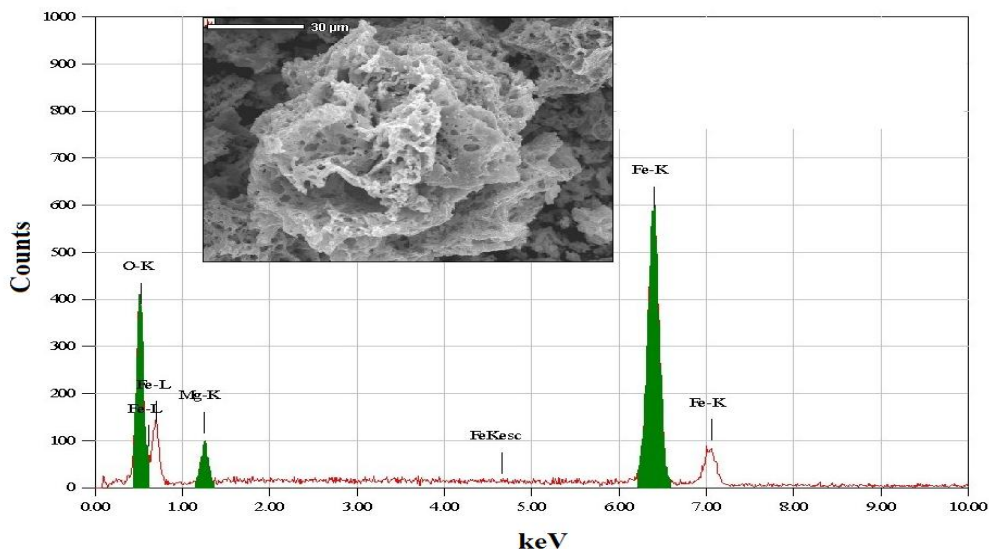


Figure 3. EDX spectrum for the as prepared sample.

Table 3 shows the relative atomic abundance of Mg, Fe and oxygen species included in the uppermost surface and bulk layers of the as synthesized sample at 20keV. This table reveals that the surface concentration of Mg species in the as synthesized sample is smaller than that in the bulk of this sample. This indicates to formation of magnesium ferrite solid solution with iron- rich composition.

Table 3. The composition of the Mg/ Fe system measured by EDX technique.

Sample	Elements	Atomic abundance (%)		Bulk Mg/Fe Ratio	Surface Mg/Fe Ratio
		Calculated (Bulk)	Found (Surface)		
MgFe ₂ O ₄ ·xFe ₂ O ₃	O	32	24.72	0.2143	0.1264
	Mg	12	08.45		
	Fe	56	66.83		

3.3.1. Homogeneity of elements

Determination of the homogeneity of elements in the as prepared sample can be achieved by using EDX technique. Fig. 4 shows the EDX patterns for the sample studied at different points.

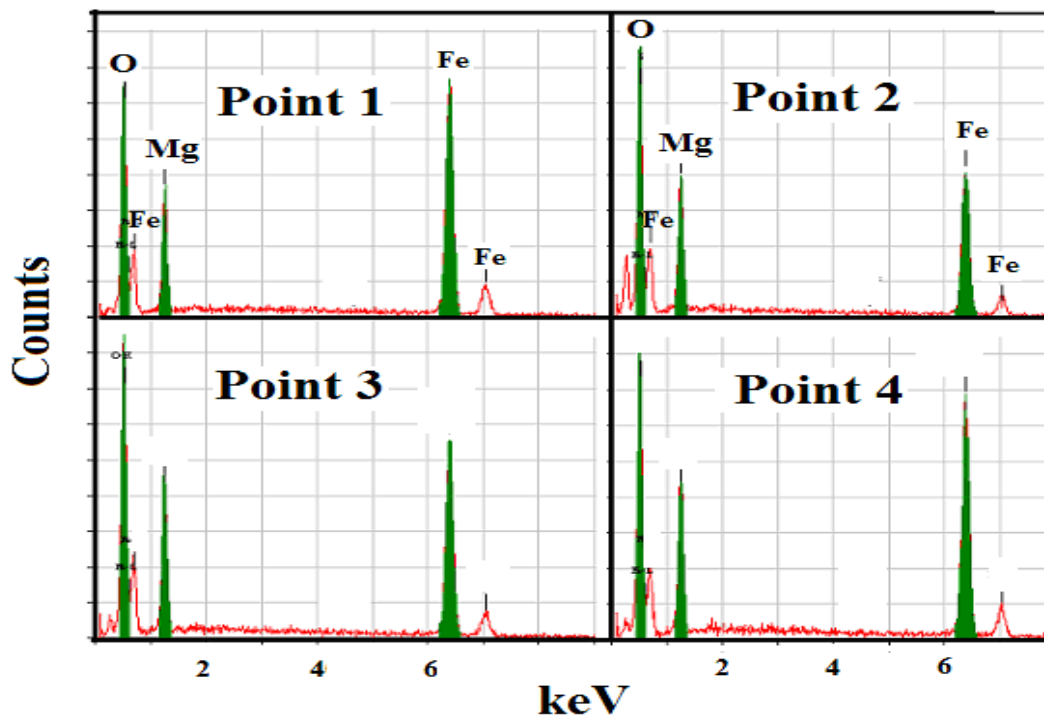


Figure 4. EDX pattern of the as prepared sample at different points.

The concentrations of O, Mg and Fe species over various points on the as prepared solid at 20 keV are summarized in Table 4. This table displays that the concentrations of O, Mg and Fe species at different points over the solid are very close to each other indicating the homogeneity of the as prepared sample.

Table 4. The atomic abundance of elements measured at 20 keV over various points on the as prepared sample.

System	Elements	Point 1	Point 2	Point 3	Point 4
MgFe ₂ O ₄ ·xFe ₂ O ₃	O	24.47	24.15	25.10	24.72
	Mg	07.61	06.52	09.80	08.45
	Fe	67.92	69.33	65.10	66.83

3.3.1. The element gradient

In addition, determination of the concentrations of O, Mg and Fe species from the uppermost surface to the bulk layers of the sample studied can be calculated using EDX technique at 5, 10, 15 and 20 keV as shown in Fig. 5.

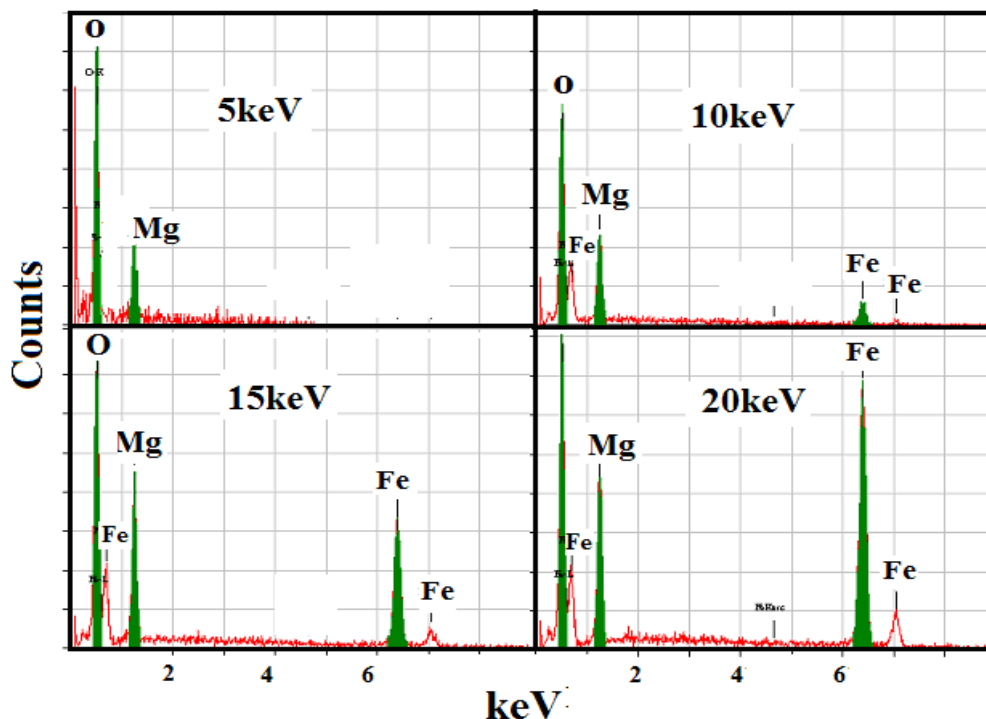


Figure 5. EDX pattern of the as prepared sample at different voltages.

The values of concentrations of O, Mg and Fe species from the uppermost surface to the bulk layers for the two investigated samples are tabulated in Table 5.

Table 5. The atomic abundance of elements measured at different voltages over the same point on the as prepared sample.

System	Elements	Atomic abundance (%)			
		5 keV	10 keV	15 keV	20 keV
MgFe ₂ O ₄ ·xFe ₂ O ₃	O	39.69	27.00	25.15	24.31
	Mg	60.31	16.37	09.95	07.12
	Fe	00.00	56.63	64.90	68.57

It can be seen from Table 5 that the surface concentrations of Mg and oxygen species for the as prepared sample decrease as the applied voltage increases from 5 to 20 keV. This means that the uppermost surface layer of the as prepared solid is O- and iron-rich layer. However, the Fe species at uppermost surface layer of the prepared sample are absent. This is observed the surface concentrations of Fe species at 5 keV. The concentration of Fe species increases as the applied voltage increase from 5 keV to 20 keV. This finding confirms that the concentration of Fe species at the uppermost surface layer is lower than that at the bulk of the as prepared sample. These observations suggest a possible

redistribution for the elements with formation of spinel magnesium ferrite solid solution with iron-rich composition.

3.4. IR analysis

IR analysis of the as prepared sample was performed; and the spectra are presented in Fig. 6. Vibrations of ions in the crystal lattice are usually observed in the range of $1000 - 400 \text{ cm}^{-1}$ in IR analysis. Two main broad metal-oxygen bands are seen in the IR spectra relative to spinel ferrite compounds. The highest one observed in the range 560 cm^{-1} , corresponds to intrinsic stretching vibrations of the metal at the tetrahedral site, whereas the lowest band usually observed in the range 410 cm^{-1} , is assigned to octahedral-metal stretching. The Mg^{2+} ions occupy mainly the octahedral sites but fraction of these ions may be migrated into tetrahedral sites. This would explain the existence of a weak shoulder in the range of $690 - 710 \text{ cm}^{-1}$. This confirms that the Mg ferrite has a partially inverse spinel structure.

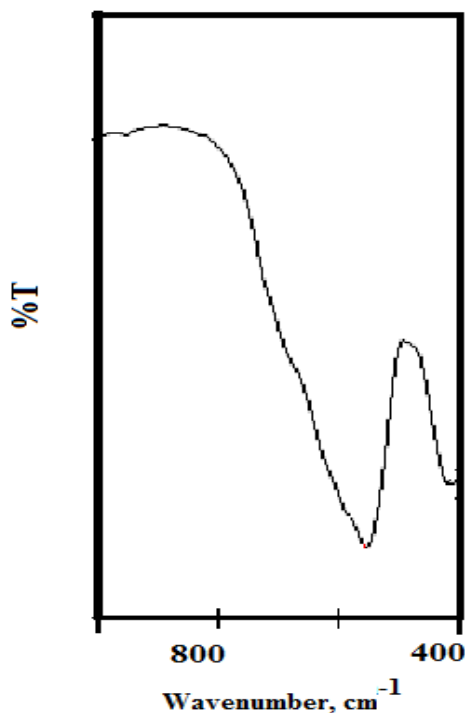


Figure 6. IR spectrum of the as prepared sample.

In fact, magnetite and its derivatives (ferrites) can be used in the coating industry, coloration, light resistance and construction industry due to their excellent alkali resistance [20- 22]. However, these compounds show potential results towards corrosion inhibition on steel due to formation of dense and stable layers of oxides. These layers act a physical barrier that protects the metal surface from corrosion [23-25]. The corrosion protection increases as the concentration of ferrite increases in high corrosion-resistant coatings [26, 27]. Ferrite based electrodes have different applications such as

various types of surface treatment, precious metal recovery, alkaline electrolytic cleaning, waste water treatment, electro-deposition coating, plating, construction and pollution treatment [28]. These applications depend upon superior physical characteristics such as low porosity and uniform crystals. Ferrite electrodes are relatively light weight. Ferrite electrodes can even be used at high voltages [27].

4. CONCLUSIONS

Formation of partially inverse spinel magnesium ferrite, $MgFe_2O_4$, solid solution with iron - rich composition has been determined. The preparation method for the investigated system is glycine - assisted combustion method. The presence of iron oxide led to formation of Mg- Fe- O solid solution containing spinel magnesium ferrite with the formula $MgFe_2O_4$. XRD, IR, SEM and EDX techniques were used for characterization of the product. The crystallite size, lattice constant, unit cell volume and X-ray density of $MgFe_2O_4$ nano- particles were calculated depending upon the data of X-ray. However, calculation of the distance between the reacting ions (L_A and L_B), ionic radii (r_A , r_B) and bond lengths (A-O and B-O) on tetrahedral (A) sites and octahedral (B) sites of the produced $MgFe_2O_4$ crystallites. These findings confirm the formation $MgFe_2O_4$ solid solution with iron - rich composition. The non-stoichiometry of magnesium ferrite nano-particles can be structurally compensated by the formation of point defects in their structure. In addition, the distribution of both Mg and Fe cations between the tetrahedral and octahedral lattice sites of the spinel structure brought about changes in the lattice parameter. The change in Mg/Fe ratio used for synthesis process led to change in the composition of the spinel nano-particles depending upon the changes in the lattice parameter of the Mg ferrite spinel. These changes in nano-particles' composition resulted in the changes at their surfaces and the properties of their interiors.

ACKNOWLEDGEMENT

This project was supported by King Saud University, Deanship of Scientific Research, College of Science Research Centre.

References

1. J.A. Toledo-Antonio, N. Nava, M. Martinez, X. Bokhimi, *Appl. Catal. A* 234 (2002) 137.
2. L. P. Li, G. S. Li, R. L. Smith Jr., H. Inomata, *Chem. Mater.* 12 (2000) 3705.
3. G. F. Goya, H.R. Rechenberg, M. Chen, W.B. Yelon, *J. Appl. Phys.* 87 (2000) 8005.
4. J. F. Hocheplied, M. P. Pileni, *J. Appl. Phys.* 87 (2000) 2472.
5. J.F. Hocheplied, P. Bonville, M.P. Pileni, *J. Phys. Chem. B* 104 (2000)905.
6. A. L. Peter (Ed.), *Pigment Handbook*, Wiley, New York, 1987.
7. R. M. Cornell, U. Schwertman, *The Iron Oxides: Properties, Reactions, Occurrence, and Uses*, VCH, Weinheim, Germany, 1996, pp. 1-25.
8. N. Pailhe', A. Wattiaux, M. Gaudon, A. Demourgues, *J. Solid State Chemistry* 181 (2008) 1040
9. P. A. Lessing, *Am. Ceram. Soc. Bull.* 68 (1989) 1002.
10. R. J. Willey, P. Noirclerc, G. Busca, *Chem. Eng. Commun.* 123(1993)1
11. Y. H. Lee, G. D. Lee, S. S. Park, S. S. Hong, *React. Kinet. Catal. Lett.* 84(2005)311

12. Y. J. Huang, J. Wang, Q. W. Chen, *Chin. J. Inorg. Chem.* 21(2005) 697
13. N.M. Deraz, A. Alarifi, *J. Analyt. Appl. Pyrolysis* 97 (2012) 55.
14. M. Kakihana, T. Okubo, M. Arima, Y. Nakamura, M. Yashima, M. Yoshimura, *J. Sol–Gel Sci. Technol.* 12 (1998) 95.
15. S. K. Biswas, D. Dhak, A. Pathak, P. Pramanik, *Mater. Res. Bull.* 43(2008)665.
16. S. V. Bangale, S. M. Khetre, S. R. Bamane, *Adv. Appl. Sci. Res.* 2(2011)252.
17. V. Bangale. Sachin, R. Bamane. Sambhaji, *Adv. Appl. Sci. Res.* 3(2011)300.
18. B. D. Cullity, *Elements of X-ray Diffraction*, Addison-Wesly Publishing Co. Inc. 1976 (Chapter 14).
19. J. A. Franco, F. C. E. Silva, *Appl. Phys. Lett.* 96 (2010) 172505.
20. Y. Liu, P. Liu, Z. Su, F. Li, F. Wen, *Dyes and Pigments* 66(2008)109.
21. Y. F. Shen, J. Tang, Z. H. Nie, Y. D. Wang, Y. Ren, L. Zuo, *Separation and Purification Technol.* 68(2009)312.
22. S. Ni, G. Zhou, F. Yang, J. Wang, Q. Wang, Deyan, *Mater. Lett.* 63(2009)2701.
23. A. Lewis, *Pigment handbook*, New York: Wiley: 758.
24. A. Kalendova, I. Sapurina, J. Stejskal, D. Vesely, *Corrosion Science* 50(2008)3549.
25. J. Brodinov, J. Stejskal, A. Kalendov, *J. Physics and Chemistry of Solids* 68(2007)1091.
26. Y. M. A. Ayana, S. M. El-Sawy, S. H. Salah, *Anti-Corrosion Methods and Materials* 44 (1997)381.
27. Sathish Reddy, B. E. Kumara Swamy, Umesh Chandra, K. R. Mahathesha, T. V. Sathisha, H. Jayadevappa, *Anal. Methods* 3(2011)2792.
28. <http://www.tdk-ninebig.com.tw/E025.PDF>